View metadata, citation and similar papers at core.ac.uk

brought to you by CORE

provided by Warwick Research Archives Portal Repository

Original citation:
Richings, Gareth and Habershon, Scott. (2017) Direct grid-based quantum dynamics on propagated diabatic potential energy surfaces. Chemical Physics Letters.

Permanent WRAP URL:
http://wrap.warwick.ac.uk/84515

Copyright and reuse:
The Warwick Research Archive Portal (WRAP) makes this work by researchers of the University of Warwick available open access under the following conditions. Copyright © and all moral rights to the version of the paper presented here belong to the individual author(s) and/or other copyright owners. To the extent reasonable and practicable the material made available in WRAP has been checked for eligibility before being made available.

Copies of full items can be used for personal research or study, educational, or not-for-profit purposes without prior permission or charge. Provided that the authors, title and full bibliographic details are credited, a hyperlink and/or URL is given for the original metadata page and the content is not changed in any way.

Publisher's statement:
© 2017, Elsevier. Licensed under the Creative Commons Attribution-NonCommercial-NoDerivatives 4.0 International http://creativecommons.org/licenses/by-nc-nd/4.0/

A note on versions:
The version presented here may differ from the published version or, version of record, if you wish to cite this item you are advised to consult the publisher's version. Please see the 'permanent WRAP URL' above for details on accessing the published version and note that access may require a subscription.

For more information, please contact the WRAP Team at: wrap@warwick.ac.uk

warwick.ac.uk/lib-publications

Direct grid-based quantum dynamics on propagated diabatic potential energy surfaces

Gareth W. Richings*, Scott Habershon*

Department of Chemistry and Centre for Scientific Computing, University of Warwick, Gibbet Hill Road, Coventry, CV4 7AL, UK

Abstract

We present a method for performing non-adiabatic, grid-based nuclear quantum dynamics calculations using diabatic potential energy surfaces (PESs) generated "on-the-fly". Gaussian process regression is used to interpolate PESs by using electronic structure energies, calculated at points in configuration space determined by the nuclear dynamics, and diabatising the results using the propagation diabatisation method reported recently [*J. Phys. Chem. A*, **119**, 12457 - 12470 (2015)]. To test this new method, the nuclear dynamics on the ground and first electronic excited states of the butatriene cation is studied using a grid-based method. The evolution of diabatic state populations is in very good agreement with those produced using a fitted potential. Overall, our scheme offers a route towards accurate quantum dynamics on diabatic PESs learnt on-the-fly.

Keywords: Direct-dynamics, Diabatisation, Grid-based quantum dynamics, Butatriene
2010 MSC: 00-01, 99-00

The study of nuclear quantum dynamics of nuclei is of great importance in helping to understand of the time-evolution of molecular systems upon excitation of the electronic degrees-of-freedom (DOFs); such simulations can make direct connections to the spectroscopy[1] and femtochemistry[2] experiments such as those pioneered by Zewail.[3–5] Quantum dynamics simulations amount to solving the time-dependent nuclear Schrödinger equation (SE) on a potential energy surface (PES) which arises due to electronic interactions. Such PESs can be model functions or generated by reference to solutions of the electronic SE. To correctly describe the dynamics of electronically excited systems, it is necessary to include multiple PESs in the calculations so as to represent the different electronic states involved. At points in nuclear configuration space where two PESs approach each other in energy, it is possible for the nuclear wavefunction to undergo non-radiative transfer between the states.[6, 7] One can model these non-adiabatic transitions using classical mechanics, as in the trajectory surface hopping (TSH) algorithm,[2, 8–10] but as the dynamics are inherently quantum mechanical, it is better to use a quantum mechanical method such as the multi-configuration time-dependent Hartree (MCTDH) approach[1, 11, 12] where possible.

The major bottleneck in performing quantum dynamics calculations is usually not the wavefunction time-propagation, but the creation of an appropriate PES on which to run the dynamics. As quantum mechanics is non-local, one needs a PES which is known everywhere in the configuration space of the nuclear motion prior to running the dynamics. For the fully quantum mechanical study of non-adiabatic systems it is usually necessary to convert the PESs from the adiabatic representation to a diabatic representation. The adiabatic representation of the potential is an energy-ordered set of PESs, and corresponds to the energies generated by electronic structure programs. However, at points in configuration space where adiabatic surfaces become degenerate, such as at conical intere-

*Corresponding author
Email addresses: G.Richings@Warwick.ac.uk (Gareth W. Richings), S.Habershon@warwick.ac.uk (Scott Habershon)

sections (CIs), there is a discontinuity in the gradient of the states, such that the adiabatic states are no longer smooth; furthermore, the coupling between the states at these points is also infinite. Neither property of the adiabatic PESs is conducive to performing wavepacket dynamics, so transformation to the diabatic representation is performed, resulting in smoothly varying surfaces with finite couplings. Diabatic representations are not unique for a given set of adiabatic states, so an appropriate diabatisation scheme must be chosen before the PES can be used in a dynamics calculation.

PESs are usually created by fitting functions to large numbers of electronic energies calculated at different points in nuclear configuration space[1, 13, 14]. Besides the amount of time it takes to perform the necessary calculations, the fitting procedure can also be very time-consuming. In order to alleviate this issue, much recent work has focussed on so-called direct-dynamics (DD) methods whereby the PESs are generated "on-the-fly" as the nuclear dynamics proceeds[15, 16]. In addition to the previously mentioned TSH method, the *ab initio* multiple spawning (AIMS) method [17–20] and the DD-variational multi-configuration Gaussian (DD-vMCG)[21–26] method have shown much success in modelling non-adiabatic dynamics. AIMS uses a wavefunction formed of a linear combination of classically-evolving Gaussian functions with quantum mechanically-evolving coefficients, whilst the DD-vMCG method takes this a step further by using quantum mechanical (rather than classical) propagation of Gaussians. The use of Gaussian wavepackets and classical trajectories is advantageous because the PES only needs to be known locally, around the centre of each Gaussian or trajectory, hence avoiding the issues of non-locality noted above. Locality is ideal for a DD method as the potential only has to be calculated at appropriate molecular geometries using an electronic structure program. However, such methods have their downsides: TSH and AIMS are limited by their classical dynamics, while DD-vMCG has numerical difficulties which arise from the non-orthogonality of the Gaussian basis functions.

Recently, we have proposed a method which combines the best elements of a DD method (*i.e.* on-the-fly generation of the PES) with the fully quantum nature and numerical stability of grid-based nuclear dynamics methods[27]. That work was restricted to a single ground-state PES, but here we extend the method to multiple electronic states using diabatic potentials generated with a propagation diabatisation scheme previously proposed by one of us.[28] In the next section we present the necessary theory behind each aspect of the method: grid-based dynamics, the method used to interpolate the PESs, and the diabatisation scheme. Subsequently, some technical details of the implementation are presented followed by results of a test calculation on the dynamics of the butatriene cation.

1. Methodology

In order to solve the nuclear time-dependent SE for a molecular system with S electronic states, we define the nuclear wavefunction as a vector of functions, $\Psi = \left(\Psi^{(1)}, \cdots, \Psi^{(S)}\right)$, each component of which represents the wavefunction moving in a particular state. The ansatz chosen for these components is a linear combination of products of time-independent basis functions along each nuclear DOF, q_κ. For state α we have [11]

$$\begin{aligned}\Psi^{(\alpha)}(\mathbf{q},t) &= \sum_{j_1}^{N_1}\cdots\sum_{j_f}^{N_f} C^{(\alpha)}_{j_1,\cdots,j_f}(t)\prod_{\kappa=1}^{f}\chi^{(\kappa)}_{j_\kappa}(q_\kappa)\\ &= \sum_J C^{(\alpha)}_J(t)\,X_J(\mathbf{q})\end{aligned} \tag{1}$$

where, for convenience, we introduce a compound index, $J = j_1, \cdots, j_f$, in the second equality. In this work, the basis functions are taken to be the point-like discrete variable representation (DVR) functions; eigenfunctions of the position operator expectation value of appropriate continuous basis functions.[11]

Using a matrix representation of the Hamiltonian (on-diagonal elements representing terms affecting only individual states and off-diagonal terms describing inter-state coupling), one can apply the Dirac-Frenkel variational principle [29, 30]

$$\langle\delta\Psi|\hat{H} - i\hbar\frac{\partial}{\partial t}|\Psi\rangle = 0, \tag{2}$$

to obtain a set of equations-of-motion (EOMs) for the wavefunction on each state[11],

$$i\hbar\dot{C}^{(\alpha)}_J = \sum_{\beta=1}^{N_s}\sum_{L=1}^{N}\langle X_J|\hat{H}^{(\alpha\beta)}|X_L\rangle\, C^{(\beta)}_L. \tag{3}$$

In order to integrate the EOMs it is necessary to be able to evaluate the Hamiltonian matrix elements. The kinetic energy contribution of the Hamiltonian is usually straightforward to evaluate, particularly in rectilinear coordinates, but in the context of a direct-dynamics approach the difficulty lies in the evaluation of the potential energy terms. The use of a DVR basis makes life easier in that the value of the integral is simply the value of the potential at the location of the grid-point [11]

$$\langle X_J|\hat{V}|X_L\rangle = V\left(\mathbf{q}_J\right)\delta_{JL}. \tag{4}$$

However, values must be known at every gridpoint, meaning that a global representation of the potential must be provided.

In this work, to generate a global representation of the potential in an "on-the-fly" manner, rather than using a precomputed PES, we employ Gaussian process regression (GPR) to approximate the potential[31–33]. In GPR, the potential is represented as a linear combination of Gaussian basis functions, $k\left(\mathbf{q},\mathbf{q}_i\right)$, each of which is centred at some point in nuclear configuration space $\mathbf{q}_i$, such that

$$k\left(\mathbf{q},\mathbf{q}_i\right) = \exp\left(-\alpha|\mathbf{q}-\mathbf{q}_i|^2\right). \tag{5}$$

The total approximation to the PES is then given by

$$V\left(\mathbf{q}\right) \approx \sum_{m=1}^{M} w^m\, k\left(\mathbf{q},\mathbf{q}_m\right). \tag{6}$$

The expansion coefficients w^m are found by solving the following set of linear equations

$$\mathbf{K}\mathbf{w} = \mathbf{b} \tag{7}$$

where $b_i = V\left(\mathbf{q}_i\right)$, the actual value of the potential at $\mathbf{q}_i$, and $K_{ij} = k\left(\mathbf{q}_i,\mathbf{q}_j\right) + \delta_{ij}\gamma^2$, the covariance between members of a reference set of M points in configuration space. The parameter, γ, is used to regularise the covariance matrix and is set to 10^{-4} in all calculations here, although the final results are quite insensitive to this parameter in this work. It is the choice of reference points which gives a particular representation of the potential; the method for choosing the reference set used here will be outlined in the next section. Finally, it is useful to define a variance function for the GPR approximation [33]

$$\sigma^2\left(\mathbf{q}\right) = 1 + \gamma^2 - \mathbf{k}^{\mathrm{T}}\mathbf{K}^{-1}\mathbf{k} \tag{8}$$

where $k_i = k\left(\mathbf{q},\mathbf{q}_i\right)$. This function, which is independent of the actual potential, gives a measure of the accuracy of the GPR representation of the potential at $\mathbf{q}$, generated by equation (6), when using a given set of reference points, $\{\mathbf{q}_i\}$.

Previously one of us published a method for generating quasi-diabatic PESs on-the-fly, within the context of DD-vMCG[28]. The approach is based on the idea of the propagation of the transformation matrix between the adiabatic and diabatic representations[34], $\mathbf{A}$, using line integrals of the non-adiabatic coupling terms (NACTs) between adiabatic states ψ_i and ψ_j,

$$\mathbf{F}_{ij} = \frac{\langle\psi_i|\nabla\hat{H}|\psi_j\rangle}{V_{jj}-V_{ii}}, \tag{9}$$

where V_{ii} and V_{jj} are the respective energies of the adiabatic states; in this expression, and those that follow, ∇ implies differentiation with respect to the nuclear coordinates. The diabatisation method relies on the approximate relationship [35]

$$\nabla\mathbf{A} \approx -\underline{\mathbf{F}}\mathbf{A}, \tag{10}$$

with the underlining indicating that $\underline{\mathbf{F}}$ is a matrix of vectors. The relationship is approximate because only a subset of all electronic states is used in practical calculations, meaning that it is not possible to totally remove inter-state coupling when diabatising the PESs. However, we are mainly interested in non-radiative transfers which occur in regions where a few (typically two) states of interest are very strongly coupled, in fact dominating the total coupling present in the system[36]. To be pragmatic, we therefore use the equation as an equality, accepting that in some regions of configuration space the diabatisation procedure is not strictly valid.

Given the transformation matrix at some point, $\mathbf{A}(\mathbf{q})$, integration of equation (10) along a path between two molecular geometries, $\mathbf{q}$ and $\mathbf{q}+\boldsymbol{\Delta}\mathbf{q}$, yields the transformation matrix at the latter point as

$$\mathbf{A}\left(\mathbf{q}+\boldsymbol{\Delta}\mathbf{q}\right) = \exp\left(-\int_{\mathbf{q}}^{\mathbf{q}+\boldsymbol{\Delta}\mathbf{q}} \underline{\mathbf{F}}\cdot\mathrm{d}\mathbf{q}\right)\mathbf{A}\left(\mathbf{q}\right). \tag{11}$$

With the transformation matrix at some molecular geometry, it is then possible to perform a similarity transform to obtain the diabatic energy matrix, $\mathbf{V}^{\mathrm{D}}$, from the adiabatic states, $\mathbf{V}^{\mathrm{A}}$,

$$\mathbf{V}^{\mathrm{D}} = \mathbf{A}^{\mathrm{T}}\mathbf{V}^{\mathrm{A}}\mathbf{A}. \tag{12}$$

It is the diabatic PESs given by this procedure which are used to perform the nuclear dynamics calculations herein.

2. Implementation

In this section, we described how the GPR approximation of a set of diabatic PESs, generated on-the-fly, is combined with an implementation of grid-based quantum dynamics. The overall methodology has been implemented in a development version of the *Quantics* nuclear quantum dynamics package, [37] such that it is compatible with quantum dynamics simulations performed using simple grid-based methods, MCTDH or DD-vMCG. Here, we focus on using a grid-based method to solve the time-dependent SE on diabatic PESs given by our GPR approach.

The quantum dynamics calculation approach here is much the same as is normally the case when using grid-based methods in the *Quantics* package; the DVR basis is defined, and initial wavefunction conditions prescribed. The multi-state DD method described here is implemented using a coordinate system of mass-frequency scaled normal modes (although it can in principle be extended to any arbitrary coordinate system). As the electronic structure calculations which are performed during the course of the dynamics are carried out using atomic Cartesian coordinates, it is necessary to provide a transformation matrix to convert between the normal modes and Cartesian coordinates. To this end, prior to the dynamics calculation, one must perform a normal mode analysis to generate the harmonic vibrational modes, their associated frequencies, and the required transformation matrix between Cartesian and normal-mode space. Usually, only a subset of normal modes is used to perform the dynamics. This subset is defined by the choice of DVR and it is the configuration subspace defined by this selection in which the GPR approximation of the PES is constructed. With regards to the GPR, we note that we used α=0.5 in all simulations reported here (see equation (5)); earlier work has shown that variation of this parameter within a reasonable range should give give little overall change in the results presented below[38].

At the start of a quantum dynamics calculation, an initial electronic structure calculation is performed at the geometry represented by the centre of the initial wavefunction. At this point, the adiabatic/diabatic transformation matrix is chosen to be the unit matrix, hence setting the global gauge of the transformation. Subsequently, 100 random geometries are chosen such that the value of each coordinate is within three standard deviations (SDs) of the centre of the wavefunction along that coordinate. The SD of the wavefunction on state α along coordinate, q_i, is defined as

$$\langle \mathrm{d}q_i^{(\alpha)} \rangle = \left(\langle \Psi^{(\alpha)} | \hat{q}_i^2 | \Psi^{(\alpha)} \rangle - \langle \Psi^{(\alpha)} | \hat{q}_i | \Psi^{(\alpha)} \rangle^2 \right)^{\frac{1}{2}}. \tag{13}$$

To maintain symmetry of the PES, according to the point group of the molecule, symmetry-equivalent geometries for the 100 random initial configurations are also defined. Electronic structure calculations are then performed at all of the chosen geometries, generating electronic energies for each state and the non-adiabatic couplings between them; all of these results are subsequently stored in a database.

With the initial set of adiabatic data, the creation of the diabatic energies at each geometry is the next step in the calculation. The calculated points are ordered in terms of increasing Euclidean distance from the central reference point; furthermore, for each reference point n, we identify of the reference point which is the nearest neighbour *and* which is also closer to the central reference point. The adiabatic/diabatic transformation matrix is then propagated out from the central reference point, each step moving to the next member in the list of proximity to the reference; in this way, the transformation matrix is approximated at all reference points. Each step of this diabatisation simply involves a numerical integration (using trapezium rule with 20 steps) of the integral in equation (11) along a straight line path between $\mathbf{q}$ and $\mathbf{q} + \Delta\mathbf{q}$. The numerator of the non-adiabatic coupling (equation (9)) is linearly interpolated between these two points, but a GPR approximation of the adiabatic energies is used to evaluate the denominator. To maintain a constant phase in the non-adiabatic couplings (a problem due to the sign indeterminacy in inter-state matrix elements, inherent in electronic structure codes), the scalar product of the numerator in equation (9) at geometries $\mathbf{q}$ and $\mathbf{q} + \Delta\mathbf{q}$ is calculated. If the result is less than zero, then the sign of the numerator at the latter geometry is switched.

After calculation of the integral, the exponential matrix in equation (11) must be formed. However, to maintain the unitarity of $\mathbf{A}$ between consecutive

points, equation (11) is rearranged as [28, 34]

$$\mathbf{A}\left(\mathbf{q}+\mathbf{\Delta q}\right)=\exp\left(\frac{1}{2}\int_{\mathbf{q}}^{\mathbf{q}+\mathbf{\Delta q}}\underline{\mathbf{F}}\cdot\mathrm{d}\mathbf{q}\right)^{-1}\times\exp\left(-\frac{1}{2}\int_{\mathbf{q}}^{\mathbf{q}+\mathbf{\Delta q}}\underline{\mathbf{F}}\cdot\mathrm{d}\mathbf{q}\right)\mathbf{A}\left(\mathbf{q}\right). \tag{14}$$

The matrix exponentials are then expanded in a Taylor series to fifth order. This resulting transformation matrix is then used to calculate the diabatic energy matrix using Eq. (12). This procedure is repeated for all reference points in the GPR approximation; having diabatised the points defining the PES, the dynamics proceeds using a GPR approimation of all elements of the diabatic energy matrix,

$$V_{ij}^{\mathrm{D}}\left(\mathbf{q}\right)\approx\sum_{m=1}^{M}w_{ij}^{m}\,k\left(\mathbf{q},\mathbf{q}_{m}\right) \tag{15}$$

The remaining aspect of our approach is the method adopted to update the reference points used by the GPR approximation to construct the diabatic PESs. With a pre-determined frequency, a new sampling of configuration space takes place to update the PES. Here, a further 100 points is randomly selected around the current wavepacket centre, using the current wavepacket SD. At each of these geometries the variance, as defined in equation (8), is calculated using the set of points calculated at earlier times to define the matrix $\mathbf{K}$ and vector $\mathbf{k}$. If the variance is greater than or equal to 10^{-6}, then a new electronic structure calculation is performed at that geometry, and this calculated energy is added to the reference set constructing the GPR approximation; if the variance is less than 10^{-6} it is assumed that the GPR approximation is sufficiently accurate at the selected geometry, and the point is discarded. As in the first step, if a new point is added to the database, then any symmetry equivalent geometries are also added. The diabatisation propagation procedure is then repeated, using all data calculated at earlier times as well as any newly added points. The old reference points are re-diabatised if any new reference points which are closer to the central reference geometry have been added. The growth of the PES continues for the duration of the dynamics; as more points are added to the database, the representation of the PES improves. In practice, we find that fewer points need to be added as the dynamics proceeds, a natural consequence of the fact that the wavefunction typically explores a finite region of space during a given propagation time.

3. Results and Discussion

To demonstrate the proposed method, test calculations were performed on the butatriene cation, a classic test case for methods in non-adiabatic dynamics[39]. Nuclear dynamics on the ground-state and first excited state of the cation have been studied using TSH[40], MCTDH[41] and DD-vMCG[22]. Furthermore, the butatriene cation was previously used to demonstrate the efficacy of the propagation diabatisation scheme outlined above[28].

Our calculations used a two-dimensional subspace of the normal modes of the ground state of the neutral butatriene molecule, as determined using complete active space self-consistent field (CASSCF) method with 6 electrons in 6 active orbitals and a 3-21G basis set. [42] The two normal modes selected to describe the nuclear dynamics, as illustrated in Fig. 1, are those representing the torsion of the molecule (labelled $5\mathrm{A}_u$ with frequency $767.6\,\mathrm{cm}^{-1}$), and the symmetric stretching of the central carbon-carbon double bond ($14\mathrm{A}_g$ with frequency $2196.2\,\mathrm{cm}^{-1}$). All necessary electronic energies and NACTs were calculated using state-averaged (SA) CASSCF(5,6)/3-21G (with equal weighting given to both electronic states). The quantum dynamics calculation used a sine DVR basis along each mode; 101 functions were used along the $5\mathrm{A}_u$ mode spanning the coordinates [-10,10], whilst 81 functions between [-8,8] were used along the totally symmetric mode, $14\mathrm{A}_g$ (the origin of this coordinate system corresponds to the Franck-Condon (FC) point). The short iterative Lanczos integrator was used to solve the EOMs. The initial wavefunction, representing the ground harmonic vibrational state, was placed on the diabatic state corresponding to the first excited adiabatic state of the cation at the FC point; it was formed as the product of Gaussian functions along each mode, centred at the origin, with no initial momentum and width of 0.7071 along each mode. The wavefunction was propagated for 100 fs with the PES reference points updated every 0.5 fs according to the algorithm outlined in the previous section. The choice of the kernel function used to construct the GPR approximation to the PES

was the two-dimensional Gaussian given in equation (5).

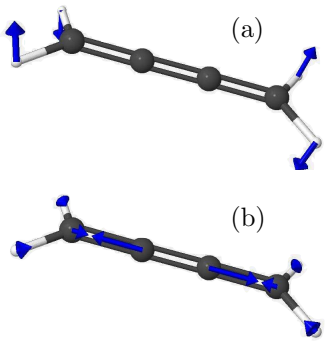

Figure 1: Pictorial representation of the normal modes of butatriene used as coordinates in this work. (a) $5A_u$: molecular torsion. (b) $14A_g$: symmetric stretching of the central C-C bond.

In Fig. 2 the PESs generated during the course of the calculation are shown: Fig. 2 (a) shows the adiabatic surfaces, while Fig. 2 (b) shows the diabatic surfaces generated by the propagation diabatisation algorithm. In total, 813 electronic structure energies were generated during propagation; we note that this represents around 10% of the total number of gridpoints used in the wavefunction propagation, demonstrating the efficiency of our "on-the-fly" interpolation approach. The conical intersection between the D_0 and D_1 adiabatic surfaces is clearly visible in the former plot at coordinates of about 2 along the $14A_g$ mode and at 0 across the $5A_u$ mode (representing a planar geometry). From Fig. 2 (b) it is clear that the diabatic surfaces cross smoothly at the location of the intersection, indicating the success of the diabatisation scheme. However, the surfaces are not perfectly smooth at the extremities of the plot. This arises as an artefact of the sampling of configuration space during the creation of the PES; only points with the space of $[-5.5, 5.5] \times [-5.5, 5.5]$ were sampled so, for the gridpoints at the edge of this space, the GPR approximation to the PESs is much less accurate. However, as the sampling is guided by the actual wavefunction dynamics, the parts of the configuration space most relevant to the dynamics are accurate.

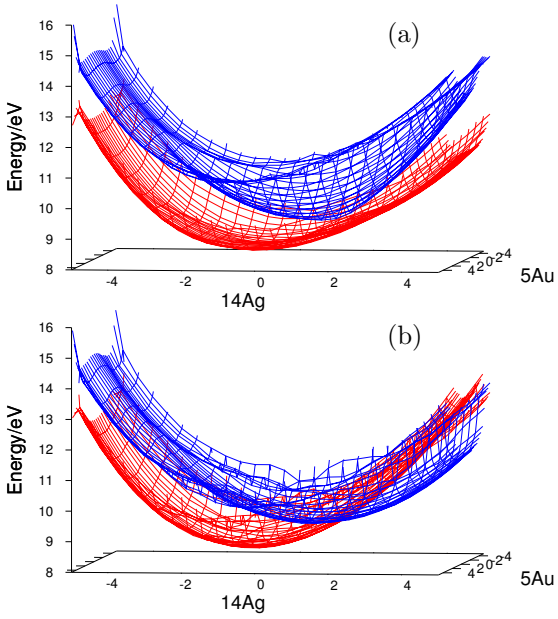

Figure 2: Potential energy surfaces of the butatriene cation calculated at the SA-CASSCF(5,6)/3-21G level using Gaussian 03 during during direct dynamics calculations as outlined in the text. (a) Adiabatic surfaces for the 2-state model. (b) Diabatic surfaces for the 2-state model.

Moving now to the actual dynamics (Fig. 3), the observable followed was the population of the $\tilde{A}$-diabatic state (corresponding to D_1 at the FC point). As a comparison to the results from the new DD method, based on SA-CASSCF, we also performed a calculation using the *fitted* PES from Ref. [41]. The comparison between the two methods is not perfect, although neither is it expected to be; the coordinate systems used in each calculation do not match exactly. As with our DD calculation, the fitted surface was constructed along the $14Ag$ stretching mode but, instead of using the normal mode representing the molecular torsion mode ($5A_u$ here), the PES was fitted as a function of the torsion angle and a periodic DVR basis used. In spite of this difference, the comparison between the two calculations is very good. The population of the $\tilde{A}$ state is plotted in Fig. 3 for both the fitted surface calculation and our grid-based DD method. Clearly, the two results are in agreement; the immediate de-population of the excited state as the intersection between the $\tilde{X}$ (corresponding to the ground state at the FC point) and $\tilde{A}$ states is encountered, complete with the brief deceleration at about 5 fs in both cases. Both plots demonstrate the partial re-population and second period of de-population between 15 and 40 fs. The two plots

correspond to one another somewhat less well at later times, but oscillation of the population between about 0.4 and 0.6 is common to both.

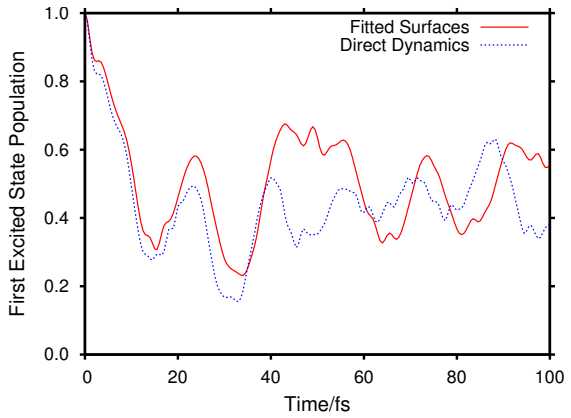

Figure 3: Wavepacket population of the first-excited, diabatic, cation state of butatriene as a function of propagation time using a two-dimensional model. The red, solid line corresponds to propagation on surfaces fitted along the $14A_g$ normal mode and along the molecular torsion angle. The blue, dashed line corresponds to propagation on surfaces generated on-the-fly (using SA-CASSCF(5,6)/3-21G) and fitted using the GPR method, with dynamics proceeding along the $5A_u$ and $14A_g$ normal modes.

Differences in the plots are to be expected of course; firstly because of the slight difference in the nature of the torsion coordinate explained above and secondly due to the form of the PES. The fitted PES was generated using the VCHAM method[41, 43, 44], a best-fit expansion in polynomials around the FC point (with additional sine functions along the torsion coordinate in this case to replicate the periodicity of the PES), and with polynomial couplings between modes and states. The GPR method approximates the PES in a similar way to an interpolation, so that the fit to points far away from the FC point is treated on the same footing as the fit at the FC point. With these small, but significant, differences it is not surprising that a sensitive measure of the dynamics such as a state population does not exactly match between the calculations, but the results are remarkably good nonetheless.

Our initial results successfully demonstrate that it is possible to perform non-adiabatic quantum dynamics calculations using a traditional grid-based method, while also generating the PES on-the-fly; the results obtained here are in very good agreement with those obtained using the more usual method of fitted surfaces. The GPR approximation provides a good approximation to the PESs and to the couplings between them, allowing replication of population transfer between the states. It should also be noted that the total time taken for the DD calculation, including the 813 electronic structure calculations, was just over 9 hours on a standard dual-core desktop.

Immediate future work will focus on interfacing the GPR method for creating multi-state PESs on-the-fly with MCTDH, allowing extension to higher-dimensional molecular systems. We note that the diabatisation method described here is also applicable to systems with more than two coupled electronic states. Further work is also required to increase the efficiency of the GPR-based method described herein, both in terms of computational time and memory requirements; however, we expect that this approach may become a useful tool for both computational and experimental researchers in the field of chemical dynamics.

Acknowledgements

This Article is dedicated to the memory of Ahmed Zewail. We are grateful to the Leverhulme Trust for funding (RPG-2016-055), and to the Centre for Scientific Computing at Warwick for providing computational resources. The data from Figs. 2 and 3 can be found at ???.

References

[1] S. Neville, G. Worth, A reinterpretation of the electronic spectrum of pyrrole: A quantum dynamics study, J. Chem. Phys. 140 (2014) 034317/1–13.

[2] M. Richter, P. Marquetand, J. González-Vázquez, I. Sola, L. González, Femtosecond Intersystem Crossing in the DNA Nucleobase Cytosine, J. Phys. Chem. Lett. 3 (2012) 3090–3095.

[3] A. H. Zewail, Femtochemistry: Atomic-scale dynamics of the chemical bond, J. Phys. Chem. A 104 (2000) 5660–5694.

[4] A. H. Zewail, Laser femtochemistry, Science 242 (1988) 1645–1653.

[5] A. Douhal, S. K. Kim, A. H. Zewail, Femtosecond molecular-dynamics of tautomerization in model base-pairs, Nature 378 (1995) 260–263.

[6] D. R. Yarkony, Diabolical conical intersections, Rev. Mod. Phys. 68 (1996) 985–1013.

[7] G. A. Worth, L. S. Cederbaum, Beyond Born-Oppenheimer: Conical intersections and their impact on molecular dynamics., Ann. Rev. Phys. Chem. 55 (2004) 127–158.

[8] J. C. Tully, R. K. Preston, Trajectory surface hopping approach to nonadiabatic molecular collisions: The reaction of H^+ with D_2, J. Chem. Phys. 55 (1971) 562–572.

[9] J. C. Tully, Molecular dynamics with electronic transitions, J. Chem. Phys. 93 (1990) 1061–1071.

[10] M. Richter, P. Marquetand, J. González-Vázquez, I. Sola, L. González, SHARC: ab Initio Molecular Dynamics with Surface Hopping in the Adiabatic Representation Including Arbitrary Couplings , J. Chem. Theory Comput. 7 (2011) 1253–1258.

[11] M. H. Beck, A. Jäckle, G. A. Worth, H. D. Meyer, The Multiconfiguration Time-Dependent Hartree (MCTDH) Method: A Highly Efficient Algorithm for Propagating Wavepackets, Phys. Rep. 324 (2000) 1–105.

[12] K. Giri, E. Chapman, C. S. Sanz, G. Worth, A full-dimensional coupled-surface study of the photodissociation dynamics of ammonia using the multiconfiguration time-dependent Hartree method , J. Chem. Phys. 135 (2011) 044311/1–13.

[13] S. Manzhos, J. Tucker Carrington, Using neural networks, optimized coordinates, and high-dimensional model representations to obtain a vinyl bromide potential surface, J. Chem. Phys. 129 (2008) 224104/1–8.

[14] W. Mizukami, S. Habershon, D. Tew, A compact and accurate semi-global potential energy surface for malonaldehyde from constrined least squares regression, J. Chem. Phys. 141 (2014) 144310/1–9.

[15] M. Persico, G. Granucci, An overview of nonadiabatic dynamics simulation methods, with focus on the direct approach versus the fitting of potential energy surfaces, Theo. Chem. Acc. 133 (2014) 1526/1–28.

[16] G. A. Worth, M. A. Robb, B. Lasorne, Solving the time-dependent Schrödinger Equation in one step: Direct Dynamics of Non-adiabatic Systems., Mol. Phys. 106 (2008) 2077–2091.

[17] M. Ben-Nun, J. Quenneville, T. J. Martínez, Ab initio multiple spawning: photochemistry from first principles quantum molecular dynamics, J. Phys. Chem. A 104 (2000) 5161–5175.

[18] M. Ben-Nun, T. J. Martínez, *Ab Initio* Quantum Molecular Dynamics, Adv. Chem. Phys. 121 (2002) 439–512.

[19] H. R. Hudock, B. G. Levine, A. L. Thompson, H. Satzger, D. Townsend, N. Gador, S. Ullrich, A. Stolow, T. J. Martínez, Ab initio molecular dynamics and time-resolved photoelectron spectroscopy of electronically excited uracil and thymine, J. Phys. Chem. A 111 (2007) 8500–8508.

[20] T. Mori, W. Glover, M. Schuurman, T. Martínez, Role of Rydberg States in the Photochemical Dynamics of Ethylene, J. Phys. Chem. A 116 (2012) 2808–2818.

[21] G. Richings, I. Polyak, K. Spinlove, G. Worth, I. Burghardt, B. Lasorne, Quantum dynamics simulations using Gaussian wavepackets: the vMCG method, Int. Rev. Phys. Chem. 34 (2015) 269–308.

[22] G. A. Worth, M. A. Robb, I. Burghardt, Non-adiabatic Direct Dynamics using Variational Gaussian Wavepackets: The $\tilde{X}/\tilde{A}$ Manifold of the Butatriene Cation, Farad. Discuss. 127 (2004) 307–323.

[23] B. Lasorne, M. A. Robb, G. A. Worth, Direct quantum dynamics using variational multi-configuration Gaussian wavepackets. Implementation details and test case., PCCP 9 (2007) 3210–3227.

[24] B. Lasorne, F. Sicilia, M. J. Bearpark, M. A. Robb, G. A. Worth, L. Blancafort, Automatic generation of active coordinates for quantum dynamics calculations: Application to the dynamics of benzene photochemistry, J. Chem. Phys. 128 (2008) 124307–10.

[25] D. Mendive-Tapia, B. Lasorne, G. Worth, M. Bearpark, M. Robb, Controlling the mechanism of fulvene S1/S0 decay: switching off the stepwise population transfer, Phys. Chem. Chem. Phys. 12 (2010) 15725–15733.

[26] D. Mendive-Tapia, B. Lasorne, G. Worth, M. Robb, M. Bearpark, Towards converging non-adiabatic direct dynamics calculations using frozen-width variational Gaussian product basis functions , J. Chem. Phys. 137 (2012) 22A548/1–10.

[27] G. Richings, S. Habershon, Potential Energy Surfaces For Nuclear Quantum Dynamics Using Gaussian Process Regression: Direct Dynamics for Grid Based Methods, In preparation, December 2016.

[28] G. Richings, G. Worth, A Practical Diabatisation Scheme for Use with the Direct-Dynamics Variational Multi-Configuration Gaussian Method, J. Phys. Chem. A 119 (2015) 12457–12470.

[29] P. Dirac, Note on Exchange phenomena in the Thomas atom, Proc. Cambridge Philos. Soc. 26 (1930) 376–385.

[30] J. Frenkel, Wave Mechanics, Clarendon Press, Oxford, 1934.

[31] A. Bartók, G. Csányi, Gaussian Approximation Potentials: A Brief Tutorial Introduction, Int. J. Quant. Chem. 115 (2015) 1051–1057.

[32] C. E. Rasmussen, C. K. Williams, Gaussian Processes for Machine Learning, MIT Press, Cambridge, Massachusetts, 2006.

[33] C. Williams, Gaussian processes, in: M. Arbib (Ed.), Handbook of Brain Theory and Neural Networks, The MIT Press, Cambridge, Massachusetts, 2002, pp. 466–470.

[34] B. Esry, H. Sadeghpour, Split diabatic representation, Phys. Rev. A 68 (2003) 042706/1–8.

[35] M. Baer, Adiabatic and diabatic representations for atom-molecule collisions: Treatment of the collinear arrangement, Chem. Phys. Lett 35 (1975) 112–118.

[36] N. Matsunaga, D. Yarkony, Energies and derivative couplings in the vicinity of a conical intersection 3. The 'most' diabatic basis, Mol. Phys. 93 (1998) 79–84.

[37] G. Worth, K. Giri, G. Richings, I. Burghardt, M. Beck, A. Jäckle, H.-D. Meyer, The Quantics Package, Version 1.1, Tech. rep., University of Birmingham, Birmingham, UK (2016).

[38] J. P. Alborzpour, D. P. Tew, S. Habershon, Efficient and accurate evaluation of potential energy matrix elements for quantum dynamics using Gaussian process regression, J. Chem. Phys. 145 (2016) 174112/1–11.

[39] L. S. Cederbaum, W. Domcke, H. Köppel, W. von Niessen, Strong vibronic coupling effects in ionization spectra: The "mystery band" of butatriene., Chem. Phys. 26 (1977) 169–177.

[40] G. Worth, P. Hunt, M. Robb, Non-adiabatic dynamics: A comparison of surface hopping direct dynamics with quantum wavepacket calculations, J. Phys. Chem. A 107 (2003) 621–631.

[41] C. Cattarius, G. A. Worth, H.-D. Meyer, L. S. Cederbaum, All mode dynamics at the conical intersection of an octa-atomic molecules: MCTDH investigation on the butatriene cation, J. Chem. Phys. 115 (2001) 2088–2100.

[42] M. J. Frisch, G. W. Trucks, H. B. Schlegel, G. E. Scuseria, M. A. Robb, J. R. Cheeseman, J. A. Montgomery, Jr., T. Vreven, K. N. Kudin, J. C. Burant,

J. M. Millam, S. S. Iyengar, J. Tomasi, V. Barone, B. Mennucci, M. Cossi, G. Scalmani, N. Rega, G. A. Petersson, H. Nakatsuji, M. Hada, M. Ehara, K. Toyota, R. Fukuda, J. Hasegawa, M. Ishida, T. Nakajima, Y. Honda, O. Kitao, H. Nakai, M. Klene, X. Li, J. E. Knox, H. P. Hratchian, J. B. Cross, V. Bakken, C. Adamo, J. Jaramillo, R. Gomperts, R. E. Stratmann, O. Yazyev, A. J. Austin, R. Cammi, C. Pomelli, J. W. Ochterski, P. Y. Ayala, K. Morokuma, G. A. Voth, P. Salvador, J. J. Dannenberg, V. G. Zakrzewski, S. Dapprich, A. D. Daniels, M. C. Strain, O. Farkas, D. K. Malick, A. D. Rabuck, K. Raghavachari, J. B. Foresman, J. V. Ortiz, Q. Cui, A. G. Baboul, S. Clifford, J. Cioslowski, B. B. Stefanov, G. Liu, A. Liashenko, P. Piskorz, I. Komaromi, R. L. Martin, D. J. Fox, T. Keith, M. A. Al-Laham, C. Y. Peng, A. Nanayakkara, M. Challacombe, P. M. W. Gill, B. Johnson, W. Chen, M. W. Wong, C. Gonzalez, , J. A. Pople, Gaussian 03, Revision D.02, Tech. rep., Gaussian Inc., Wallingford CT (2004).

[43] H. Köppel, W. Domcke, L. S. Cederbaum, Multimode molecular dynamics beyond the Born-Oppenheimer approximation, Adv. Chem. Phys. 57 (1984) 59–246.

[44] L. S. Cederbaum, H. Köppel, W. Domcke, Multimode vibronic coupling effects in molecules, Int. J. Quant. Chem. 15 (1981) 251–267.